Organic Semiconductor Bulk Heterojunction Thin Films

by Chris Berger

Soluble organic semiconductors suitable for spin-cast, reel-to-reel, and inkjet deposition promise to greatly reduce the manufacturing cost of devices such as solar cells and LEDs. This paper provides an overview of efforts to create flourene-based bulk heterojunction thin films suitable for solar cells and compares how various manufacturing methods and parameters affect electronic and morphologic properties.

Table of Contents

Introduction

Ever-increasing energy consumption by the world's population is driving research into renewable energy sources, such as electricity generation by solar cells. While conventional semiconductors, such as group-4 (silicon), III-V (GaAs), and II-VI (CdTe) have played an important role, they remain cost-prohibitive when compared to fossil fuels. [1] Organic semiconducting materials are capable of being deposited in solution on inexpensive substrates, as opposed to expensive Bridgeman growth of bulk silicon crystals or vacuum deposition of CdTe films, for example. Therefore, organic semiconductors could provide cost-effective renewable energy. [2] However, various challenges remain in achieving sufficient efficiencies in devices compatible with inexpensive manufacturing processes.

Heterojunctions

In organic photovoltaic solar cells, the semiconducting material absorbs photons of compatible wavelength. This action generates electron-hole pairs, i.e. an electron

from the HOMO is promoted to the LUMO, leaving behind a hole in the HOMO. A force – generally an electric field – drives the electrons and holes to opposite ends of the semiconducting material, where they are drawn out by conducting contacts. If the mobility of the holes and electrons is low, however, then they may recombine before reaching the electrodes; this results in no electrical energy generation (Figure 1).

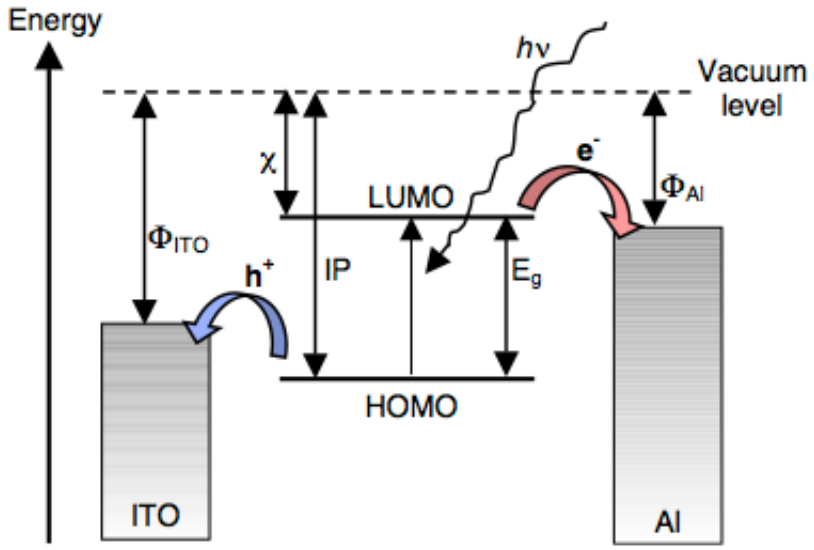

Figure 1 – Energy extraction from organic semiconductor solar cell with Al and ITO electrodes. [2]

In the case of solar cells, the driving force for charge separation is not provided by an external circuit (biasing), but is instead provided by the work function of the two electrodes. When the two electrodes are connected, their work functions equalize, but the LUMO and HOMO levels of the semiconductor bend due to Fermi level pinning (Figure 2). This provides the field that drives carriers to the electrodes and produces electricity.

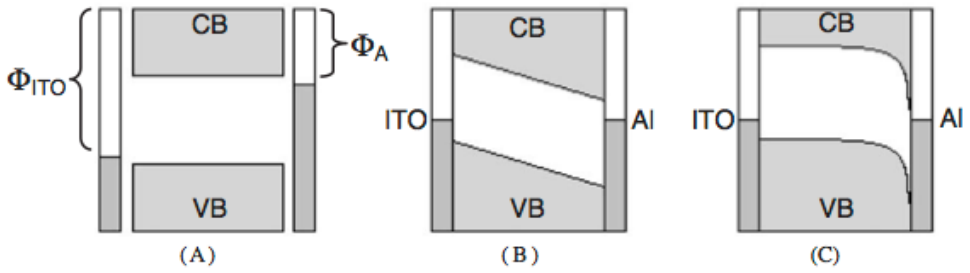

Figure 2 – Band bending of the semiconductor HOMO and LUMO when contacted by ITO and Al electrodes. In this example, the semiconducting material is p-type (a Schottky junction). [2]

Bilayer vs. Bulk Heterojunctions

In a bilayer heterojunction, two different semiconducting materials are deposited on a substrate in distinct layers. Each material has different LUMO and HOMO levels, which increases the charge separating force (Figure 3).

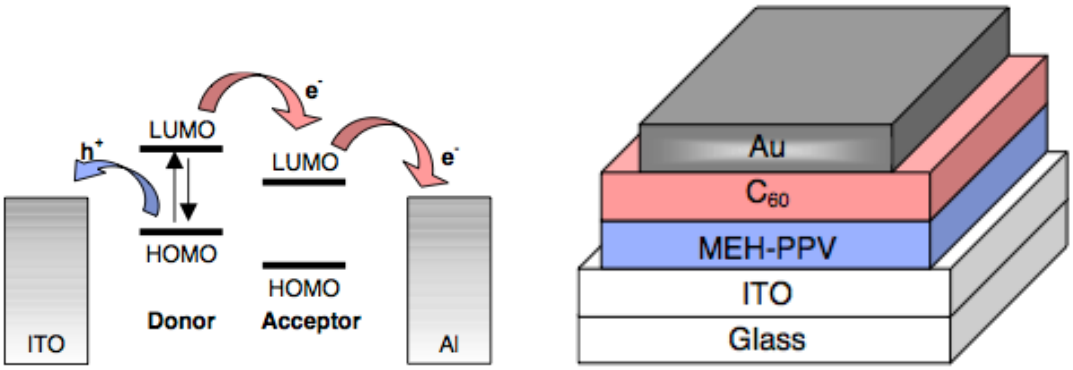

Figure 3 - Charge separation mechanism in a bi-layer organic photovoltaic device. The electron-accepting C60 layer drives electrons to the Au contact while the donating MEH-PPV layer drives holes to the ITO electrode. [2]

The inherent problem with organic bilayer heterojunction photovoltaic devices is that, generally speaking, the diffusion length of excitons (bound electron-hole pairs) is limited to about 10 nm. However, a 20 nm bilayer heterojunction is far too thin to

absorb a meaningful amount of solar radiation due to insufficient absorption coefficients. [3]

The solution to this issue is to blend the two semiconducting materials in such a way that they form phase-separate interfaces at the nanoscale throughout the bulk of the semiconductor. In this way, most excitons form just a few nm away from an interface, driving charge separation and ultimately electricity generation (Figure 4).

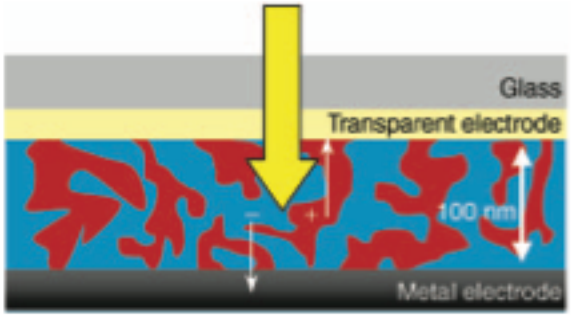

Figure 4 – Typical bulk heterojunction schematic. The HTM and ETM organic semiconductors mix to form nanoscale regions of donating and accepting regions. The red donor region has high hole mobility, so holes that reach the red region quickly drift toward the transparent electrode. The blue acceptor region has high electron mobility, so electrons that reach the blue region quickly drift toward the metal electrode. [3]

Figure 5 shows another schematic representation of the process of charge separation in bulk heterojunctions with an arbitrary mixing profile. The left diagram shows a film cross section while the right diagram shows the energy profile of the HTM and ETM semiconductors and the ITO and Al electrodes.

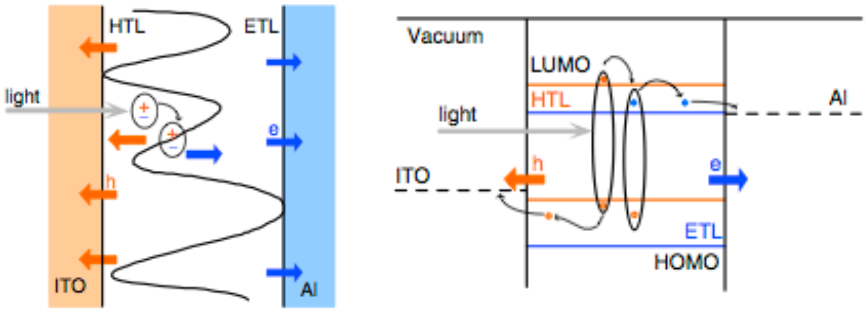

Figure 5 – charge separation and energy diagram of bulk heterojunction PV device. [4]

Studies of Bulk Heterojunction Growth

It follows from the previous section that the best performing bulk heterojunction is obtained when the semiconductor constituent phase separation is of the order of the diffusion length of the excitons, and the material forms a bicontinuous network allowing movement of the carriers to the collecting electrodes. [5] Blend ratios, deposition temperature, annealing processes, and film thickness, among other attributes, strong affect film morphology. Getting these parameters right is critical to creating high quality films. The next sections focus on efforts to create a variety of bulk heterojunction devices by optimizing these and other parameters.

ETM and HTM Blending

Considerable effort has been exerted [6] [7] [8] [3] [9] [10] [11] [12] [13] [14] [15] [16] determining the optimum ratio of hole transporting and electron transporting semiconductor constituents to maximize solar cell performance.

In order to determine the best ratio, researchers spin-cast the soluble constituents onto a glass substrate with evaporated electrodes, with a typical structure shown in

Figure 6. The blend is formed by solvent-quenching, in which the polymers are dissolved in a common solvent and form a homogeneous solution, which phase separates when the solvent evaporates from the solution. [4] The transparent conductive layer is typically ITO, the transparent conductive polymer is typically PEDOT:PSS, the interface layer is typically LiF and the metal electrode is typically aluminum.

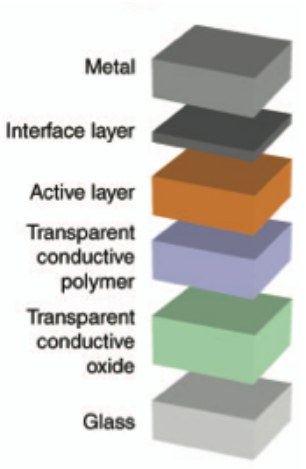

Figure 6 – Typical architecture for organic bulk heterojunction solar cell. [3]

In 2005, Reyes et. Al [6] conducted a study of P3HT:PCBM blend films. The authors found that by adjusting the ratio of P3HT to PCBM, they were able to optimize the solar spectrum absorption characteristics (Figure 7).

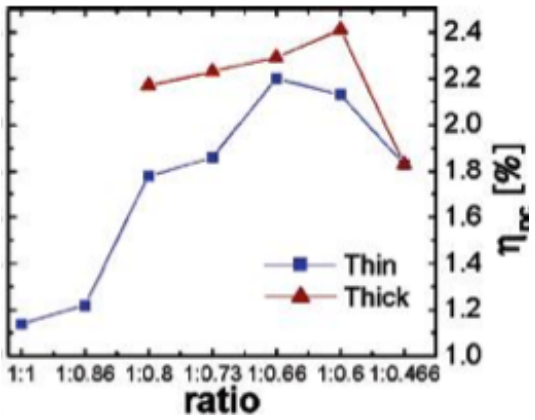

Figure 7 – Affect of PCBM to P3HT ratio (and film thickness) on solar spectrum energy conversion efficiency.

Halls, et Al. [7] performed studies on bulk heterojunction blends of MEH-PPV:CN-PPV. Using different ratios of MEH-PPV:CN-PPV, the authors found that the composition range of 1:4 to 4:1 by weight would provide good charge separation. Electron micrographs show distinct constituent phase separation (Figure 8).

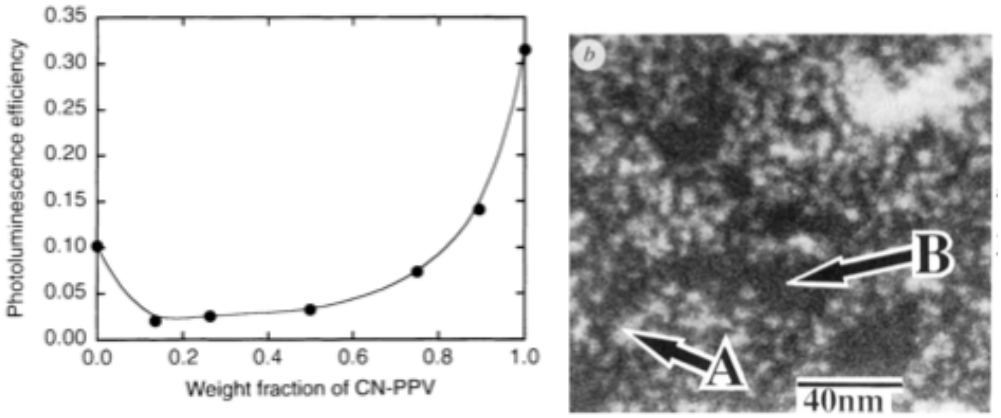

Figure 8 – Left: Charge separation efficacy vs. CN-PPV ratio. Note that this chart shows "photoluminescent efficiency", which is the efficiency by which charges recombine radiatively. So, a lower value represents better performance in a solar cell. Right: Light areas represent CN-PPV microcrystals and dark regions represent MEH-PPV microcrystals.

Kim, et. Al. [9] report spin-casting P3HT:F8BT bulk heterojunctions. The authors found that a weight ratio of 60:40 of P3HT:F8BT gave the highest external quantum efficiency (Figure 9).

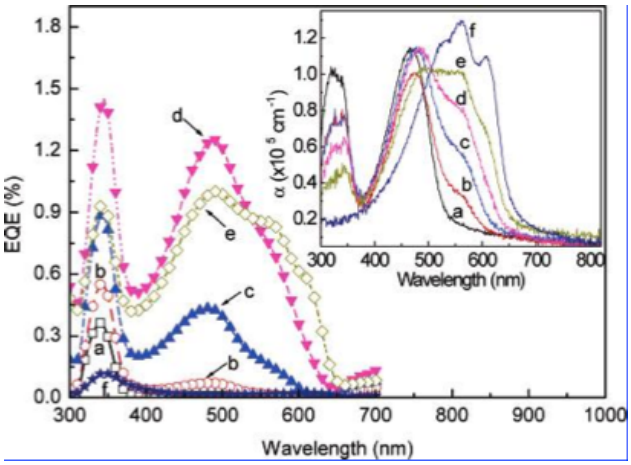

Figure 9 – External Quantum Efficiency (EQE) of various P3HT:F8BT ratios. 60:40 is labeled "d". [9]

Snaith, et. Al. [10] have performed studies on PFB:F8BT bulk heterojunction films with three different forms of F8BT: F8BT69, F8BT129, and F8BT188. They found the best performing films around a ratio of 5:1 PFB:F8BT (Figure 10).

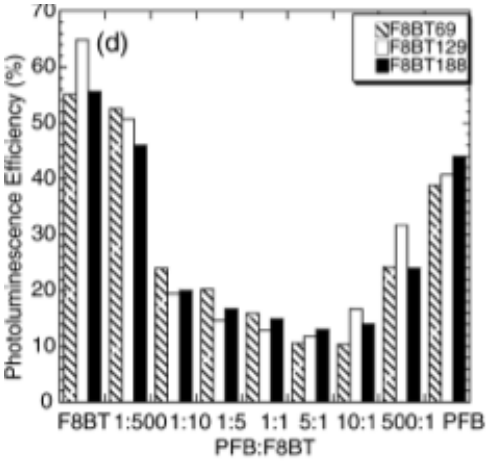

Figure 10 – Photoluminescent Efficiency of PFB:F8BT blends. [10]

Film Morphology

The ratio of blend constituents affects the microstructure of the film. [4] The difference in device performance for various blend ratios has been attributed to changes in the microstructure characteristics. [11]

For example, in [16], AFM was performed on PFB:F8BT blend films with ratios 1:5, 1:1, and 5:1 (Figure 11). The authors speculate that the relative size of crystallites doesn't matter nearly as much as the total PFB:F8BT interface area, because only excitons generated within a few nm of an interface are likely to undergo charge separation prior to recombination. Shikler, et. Al. [11] reached a similar conclusion (Figure 12).

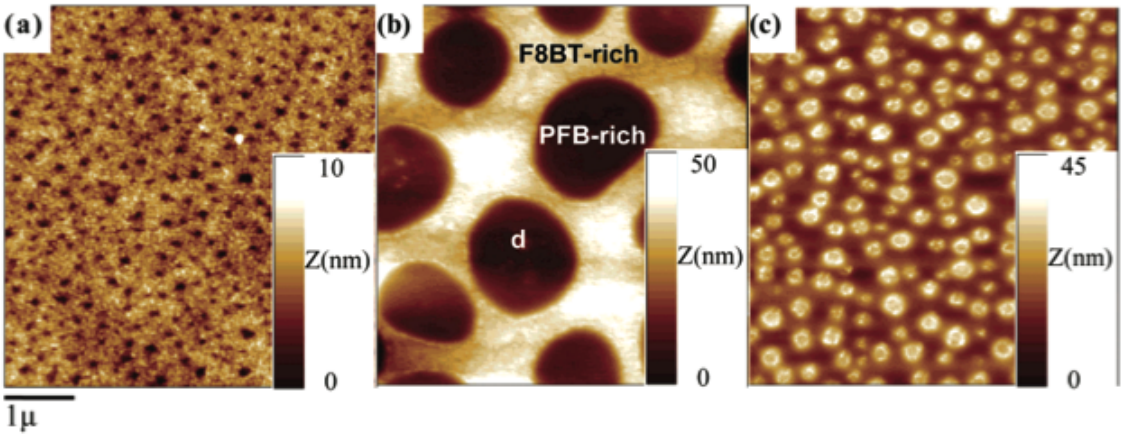

Figure 11 – ATF images for PFB:F8BT thin films of various blend ratios (a=1:5, b=1:1, c=5:1). [16]

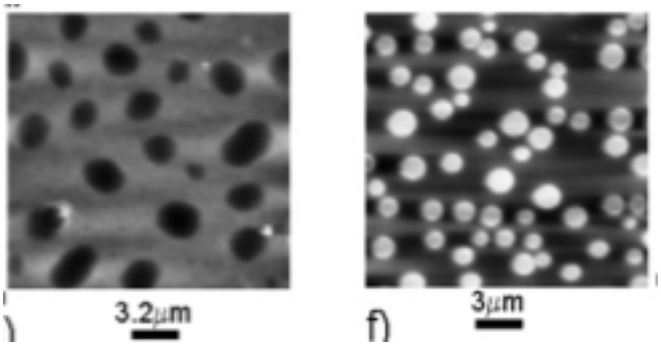

Figure 12 – ATF of 5:1 (left) and 1:5 (right) PFB:F8BT films. [11]

Xia, et. Al. [14] take this a step further and propose a TFB:F8BT film formation model consisting of four phases: an F8BT phase, a TFB phase, and bilayers of F8BT on TFB and TFB on F8BT (Figure 13). The authors postulate that the more bilayers that are formed, the better the device performance; however, this particular paper does not investigate bilayer formation with respect to blend ratios.

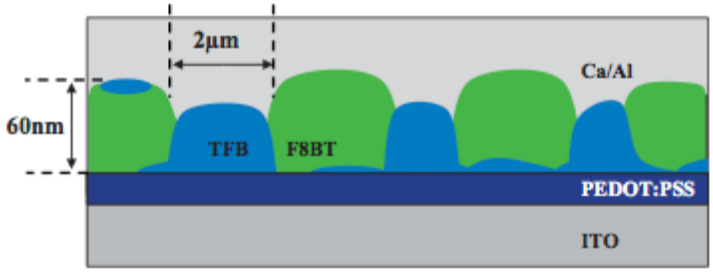

Figure 13 – Proposed structural model of TFB:F8BT film. [14]

Kim, et. Al. [13] propose a similar model of TFB:F8BT film formation, although they argue that TFB fully wets the entire PEDOT:PSS surface, such that a pure F8BT phase from PEDOT:PSS to the Aluminum electrode is not possible (Figure 14).

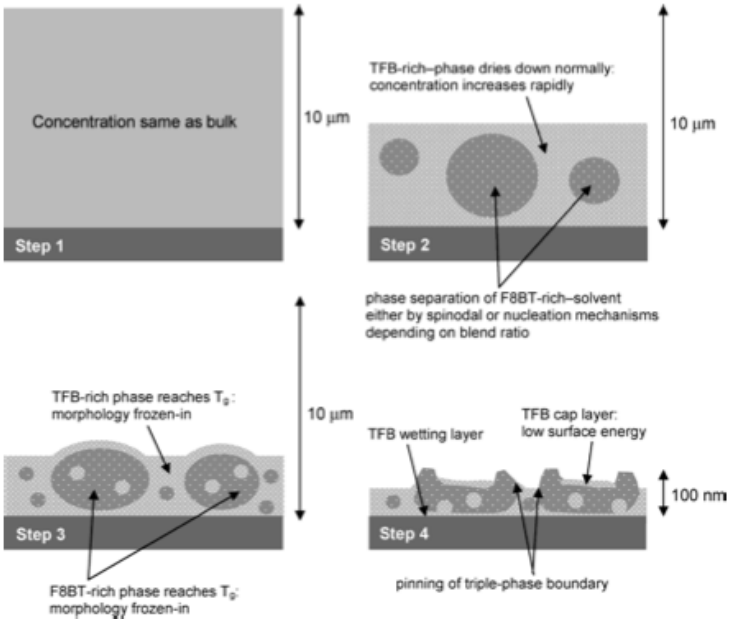

Figure 14 – Proposed growth model for TFB:F8BT bulk heterojunction thin film. [13]

Finally, Mayer, et. Al. [17] performed x-ray diffraction on a variety of polymer-fullerene BHJ films and determined the optimum mixing ratio for a variety of polymer:PCBM materials. The authors propose intercalation mechanisms for various ratios and how specific ratios result in specific intercalation formations and how this affects solar cell performance (Figure 15).

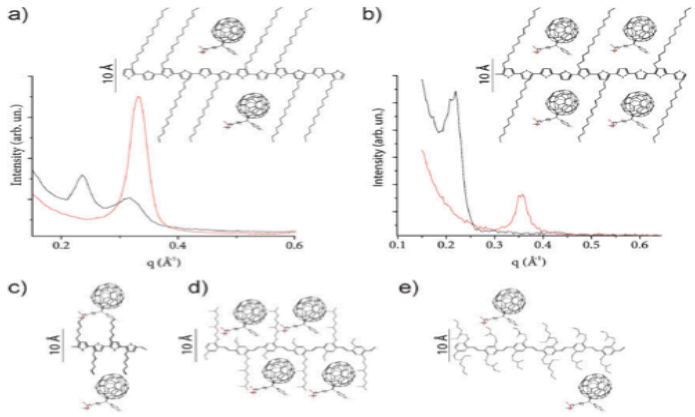

Figure 15 – Polymer:Fullerene intercalation for various polymers.

Conclusion

This paper has discussed the physics of organic semiconductor photovoltaic solar cell operation principles. We have explored the differences between bilayer and bulk heterojunctions, and concluded that due to the extremely short electron and hole free carrier diffusion lengths in organic semiconductor films, bulk heterojunctions seem to carry an advantage over bilayer planar heterostructures due to the increased interfacial area and smaller average distance from excitons generation to n-p interface. We looked at several papers where the hole-transporting and electron-transporting semiconducting material ratios were optimized to give the best device performance, and then examined atomic force micrographs and proposed growth models to explore possible mechanisms that lead to certain film ratios performing better than others.

Bibliography

[1] Jenny Nelson, *The Physics of Solar Cells*. London: Imperial College Press, 2003.

[2] Holger Spanggaard and Frederik Krebs, "A brief history of the development of organic and polymeric photovoltaics," *Solar Energy Materials and Solar Cells*, vol. 83, pp. 125-146, 2004.

[3] Rene A.J. Janssen, Jan C. Hummelen, and N. Serdar Sariciftci, "Polymer-Fullerene Bulk Heterojunction Solar Cells," *MRS Bulletin*, vol. 30, pp. 33-36, 2005.

[4] Ellen Moons, "Conjugated polymer blends: linking film morphology to performance of light emitting diodes and photodiodes," *Journal of Physics: Condensed Matter*, vol. 14, pp. 12235-12260, 2002.

[5] David Jones, "Flourene-Containing Polymers for Solar Cell Application," in *Organic Photovoltaics: Materials, Device Physics, and Manufacturing Technologies*, Christoph Brabec, Vladimir Dyakonov, and Ullrich Scherf, Eds. Weinhein, Germany: Wiley-VCH, 2008, pp. 57-92.

[6] Marisol Reyes-Reyes et al., "Meso-Structure Formation for Enhanced Organic Photovoltaic Cells," *Organic Letters*, vol. 7, no. 26, pp. 5749-5752, 2005.

[8] Marc Koetse, Jorgen Sweelssen, Kornel Hoekerd, and Herman Schoo, "Efficient polymer:polymer bulk heterojunction solar cells," *Applied Physics Letters*, vol. 88, pp. 083504 1-3, 2006.

[7] J.J.M. Halls et al., "Efficient Photodiodes from Interpenetrating Polymer Networks," *Nature*, vol. 376, pp. 498-500, 1995.

[9] Youngkyoo Kim et al., "Organic Photovoltaic Devices Based on Blends of Regioregular Poly(3-hexylthiophene) and Poly(9,9-dioctylfluorene-co-benzothiadiazole)," *Chemistry of Materials*, vol. 16, pp. 4812-4818, 2004.

[10] Henry Snaith and Richard H. Friend, "Morphological dependence of charge generation and transport in blended polyfluorene photovoltaic devices," *Thin Solid Films*, vol. 451, pp. 567-571, 2004.

[11] Rafi Shikler, Marco Chiesa, and Richard H. Friend, "Photovoltaic Performance and Morphology of Polyfluorene Blends: The Influence of Phase Separation Evolution ," *Macromolecules*, vol. 39, pp. 5393-5399, 2006.

[12] Henry J. Snaith, Neil C. Greenham, and Richard H. Friend, "The Origin of Collected Charge and Open-Circuit Voltage in Blended Polyfluorene Photovoltaic Devices," *Advanced Materials*, vol. 16, no. 18, pp. 1640-1645, 2004.

[13] Ji-Seon Kim, Peter K. H. Ho, Craig E. Murphy, and Richard H. Friend, "Phase Separation in Polyfluorene-Based Conjugated Polymer Blends: Lateral and

Vertical Analysis of Blend Spin-Cast Thin Films ," *Macromolecules*, vol. 37, pp. 2861-2871, 2004.

[14] Yajun Xia and Richard H. Friend, "Phase Separation of Polyfluorene-Based Blend Films and Its Influence on Device Operations ," *Advanced Materials*, vol. 18, pp. 1371-1376, 2006.

[15] C. M. Bjorstrom and Magnusson E. Moons, "Control of phase separation in blends of polyfluorene (co)polymers and the C60-derivative PCBM," *Synthetic Metals*, vol. 152, pp. 109-112, 2005.

[16] Henry J. Snaith, Ana C. Arias, Arne C. Morteani, Carlos Silva, and Richard H. Friend, "Charge Generation Kinetics and Transport Mechanisms in Blended Polyfluorene Photovoltaic Devices," *Nano Letters*, vol. 2, no. 12, pp. 1353-1357, 2002.

[17] A. C. Mayer et al., "Bimolecular Crystals of Fullerenes in Conjugated Polymers and the Implications of Molecular Mixing for Solar Cells," *Advanced Functional Materials*, vol. 19, pp. 1173-1179, 2009.